DOI: 10.21857/94kl4cepvm

Pregledni članak / Review paper
Prihvaćeno / Accepted: 15. svibnja 2025.

THE HYDROTHERMAL SYNTHESIS OF NANOMATERIALS

Stanislav Kurajica, Katarina Mužina

Abstract

Nanomaterials can be prepared by means of various synthesis methods, such as sol-gel synthesis, combustion synthesis, mechanochemical synthesis, etc. Among numerous nanosynthesis methods, hydrothermal synthesis is one of the most commonly used. Hydrothermal/solvothermal reaction is defined as a chemical reaction that occurs in a closed reaction vessel above the boiling point of water/solvent. The development of hydrothermal techniques has a history of more than 150 years, starting from the synthesis of macro crystals, through the synthesis of conventional materials, all the way to the synthesis of new advanced materials, particularly nanomaterials. In this paper, the setup of hydrothermal experiment and the procedure of hydrothermal synthesis are described. Furthermore, the parameters available for process control, as well as advantages and disadvantages of the hydrothermal synthesis, are discussed. Finally, a brief overview of the first author scientific group achievements in hydrothermal synthesis of ceria is presented.

Keywords: hydrothermal synthesis; nanomaterials; ceria.

1. INTRODUCTION

Intensive investigation of various nanomaterials, their synthesis, properties and utilization in various areas has been carried out over approximately last 50 years. Considerable progress and substantial impact of these efforts on science, economy and society has been noted as a result thereof. Nanomaterials enabled many improvements, providing advanced materials, industrial products, electronics, sporting goods, consumer products, diagnostic and therapeutic procedures, environmental applications, renewable energy solutions, etc. [1,2]. According to the Royal Society and the Royal Academy of Engineering [3], nanotechnology is the design, characterization, production and application of structures, devices and systems by controlling the shape and size at the nanom-

eter scale. Therefore, crucial features of nanotechnology are dimensions, i.e. at least one dimension below 100 nm, and fundamentally new properties, different from the properties of parent bulk materials, due to nano dimensions [1]. According to dimensions, nanomaterials can be classified into [4]: 0-dimensional, having all three dimensions below 100 nm, such as quantum dots [5], metal [6] and semiconductor nanoparticles (Fig. 1) [7], etc.; 1-dimensional, with two dimensions on the nanoscale, such as nanorods [8], nanowires [9], nanotubes (Fig. 2) [10], etc.; 2-dimensional, with only one dimension below 100 nm, such as nano-coatings [11], thin films (Fig. 3) [12], layered materials, etc.; and 3-dimensional, without any dimensions on the nanoscale, but being nanostructured such as nanocrystalline glass-ceramics (Fig. 4) [13], metallic glasses [14], composite materials, etc. Therefore, nanotechnology does not deal with nanoparticles only. Nanotechnology has made it possible to integrate nanoparticles into macroscopic systems of nano- to macroscopic sizes. Nanotechnology empowered the manufacturing of nanostructured materials having elements with one or more dimensions on the nanoscale. Nanotechnology enabled the creation of nanodevices, relatively simple devices able to perform simple tasks, such as sensors or transducers, capable of converting energy from one form to another, storing information, etc. Finally, nanotechnology has created systems of great sophistication and complexity, capable of performing complex tasks, such as information processing [1]. Although nanotechnology is much more than nanoparticles, their production and use still remains an important sector of nanotechnology. In a recent review, Kumari et al. [15] called nanoparticles the foundation of nanotechnology.

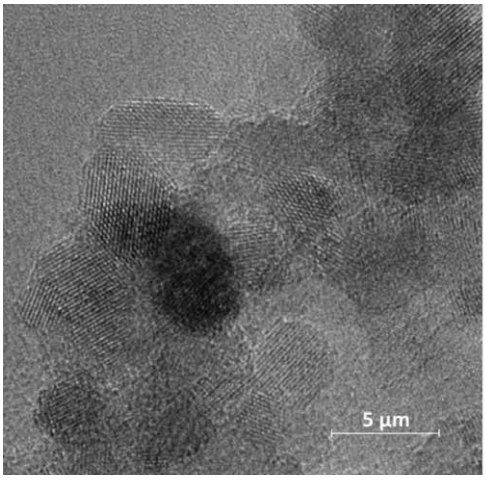

Figure 1. HRTEM micrograph of the hydrothermally derived anatase nanoparticles (0D nanomaterial). (Reprinted from the publication: S. Kurajica, I. Grčić, I. Minga, V. Mandić, K. Mužina, Hydrothermally-Derived Silver-Decorated Nanocrystalline Anatase Photocatalyst for Reactive Violet 2 Photodegradation, Processes, 11 (2023) 210. CC-BY-4.0.)

Slika 1. HRTEM mikrografija anatasa dobivenog hidrotermalnim postupkom (0D nanomaterijal). (Pretisnuto iz publikacije: S. Kurajica, I. Grčić, I. Minga, V. Mandić, K. Mužina, Hydrothermally-Derived Silver-Decorated Nanocrystalline Anatase Photocatalyst for Reactive Violet 2 Photodegradation, Processes, 11 (2023) 210. CC-BY-4.0.)

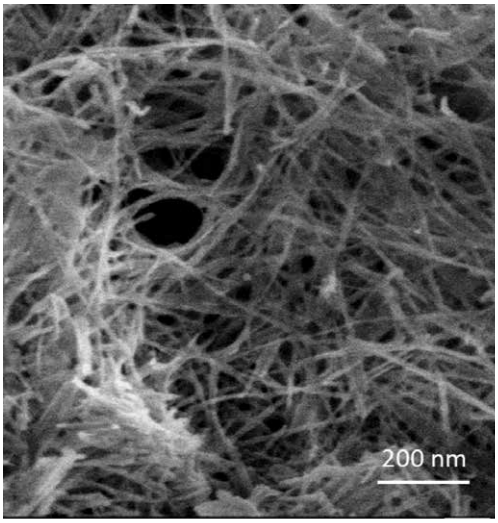

Figure 2. FESEM micrograph of titanate nanotubes (1D nanomaterial). (Reprinted from the publication: S. Kurajica, J. Macan, V. Mandić, M. Galjer, K. Mužina, J. R. Plaisier, Reinforcing blade-cast photocatalytic titania thin film by titanate nanotubes, Materials Research Bulletin, 105 (2018) 142-148. Copyright (2018), with permission from Elsevier.)

Slika 2. FESEM mikrografija titanatnih nanocjevčica (1D nanomaterijal). (Pretisnuto iz publikacije: S. Kurajica, J. Macan, V. Mandić, M. Galjer, K. Mužina, J. R. Plaisier, Reinforcing blade-cast photocatalytic titania thin film by titanate nanotubes, Materials Research Bulletin, 105 (2018) 142-148. Copyright (2018), s dopuštenjem Elseviera.)

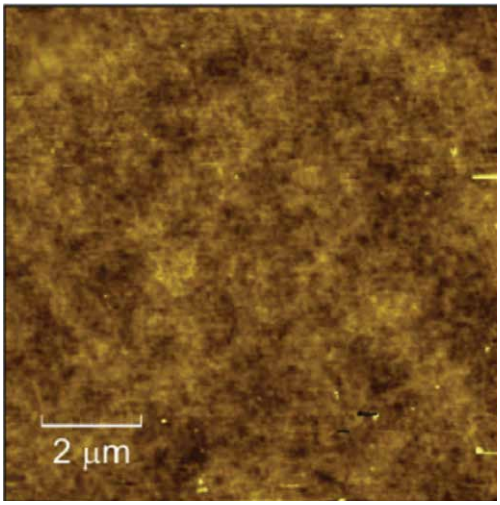

Figure 3. AFM micrograph obtained in a dynamic scanning mode depicting the monolayer thin-film (2D nanomaterial) at the surface of of thermal insulation glass, average thickness approximately 28 nm, surface roughness of about 4 nm. (Reprinted from the publication: V. Mandić, S. Kurajica, I. Panžić, A. Bafti, J. Šipušić, K. Mužina, F. Brleković, L. Gigli, M. Gaboardi, Utilization of conventional PXRD apparatus for characterization of thin-films using reconsidered equations for XRD, Surfaces and Interfaces, 36 (2023) 102554. Copyright (2023), with permission from Elsevier.)

Slika 3. AFM mikrografija dobivena uz dinamički način pretraživanja koja prikazuje jednoslojni tanki film (2D nanomaterijal) na površini termoizolacijskog stakla, prosječna debljina približno 28 nm, površinska hrapavost oko 4 nm. (Pretisnuto iz publikacije: V. Mandić, S. Kurajica, I. Panžić, A. Bafti, J. Šipušić, K. Mužina, F. Brleković, L. Gigli, M. Gaboardi, Utilization of conventional PXRD apparatus for characterization of thin-films using reconsidered equations for XRD, Surfaces and Interfaces, 36 (2023) 102554. Copyright (2023), s dopuštenjem Elseviera.)

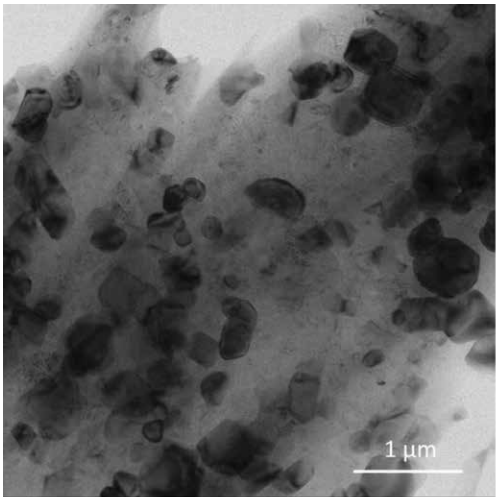

Figure 4. Bright field HRTEM micrographs of glass-ceramics (3D nanomaterial). (Reprinted from the publication: S. Kurajica, J. Šipušić, M. Zupancic, Igor Brautović, M. Albrecht, $ZnO\text{-}Al_2O_3\text{-}SiO_2$ glass ceramics: Influence of composition on crystal phases, crystallite size and appearance, J Non-Cryst. Solids, 553 (2021) 120481. Copyright (2021), with permission from Elsevier.)
Slika 4. HRTEM mikrografija u svijetlom polju uzorka staklokeramike (3D nanomaterijal). (Pretisnuto iz publikacije: S. Kurajica, J. Šipušić, M. Zupancic, Igor Brautović, M. Albrecht, $ZnO\text{-}Al_2O_3\text{-}SiO_2$ glass ceramics: Influence of composition on crystal phases, crystallite size and appearance, J Non-Cryst. Solids, 553 (2021) 120481. Copyright (2021), s dopuštenjem Elseviera.)

2. NANOMANUFACTURING

Nanomanufacturing techniques are most frequently classified into top-down and bottom-up methods. Top-down are techniques of removing aggregates of molecules from the surface of a bulk material, while bottom-up are techniques of assembling and arranging individual atoms or molecules using chemical and physical interactions that allow components to be arranged in an ordered manner into nanostructures [1]. A simplified schematic representation of both processes is shown in Figure 5. It could be argued that top-down techniques are predominantly of physical nature, while bottom-up techniques are based on chemical processes [2], although this is not entirely true. However, nanomanufacturing processes can indeed be divided into those of a predominantly physical nature (without a chemical reaction) and those of a predominantly chemical nature (with a chemical reaction). Another approach classifies the nanomanufacturing techniques into nanoparticle production methods and nanostructured materials production methods [1]. Recently, molecular nanofabrication methods and nanobiotechnological methods are gaining in importance. The top-down approach is currently dominant in industrial applications owing to the utilization of numerous methods, from grinding for the production of nanoparticles to lithography used for microprocessors manufacturing [15]. However, in chemical laboratories, the bottom-up approach is far more common.

This group of methods implies the building of nanomaterials from the smallest units, such as atoms or molecules [16]. This approach allows building of aimed sizes and shapes, and has the potential to be more cost-effective and produce less waste [15]. Even when focusing only on chemical methods, which the authors find more convenient, the methods remain numerous and diverse, from the simple chemical synthesis [12] and the slightly more complex wet chemical techniques [9,11] up to the methods for the preparation of nanostructured materials [13].

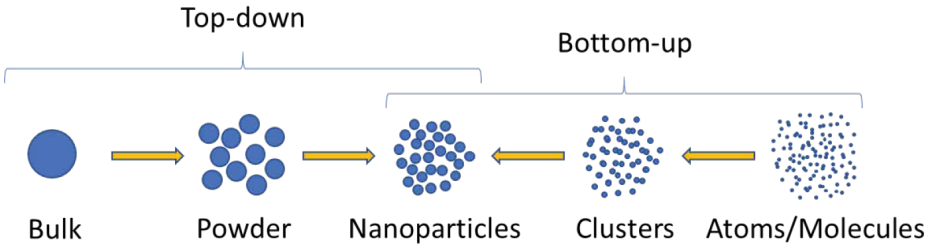

Figure 5. Schematic representation of top-down and bottom-up nanomanufacturing approaches.
Slika 5. Shematski prikaz pristupa nanoproizvodnji odozgo prema dolje i odozdo prema gore.

There is no ideal method of materials synthesis, some involve precursors or solvents harmful to the environment, some require valuable equipment or expensive chemicals, high temperatures or pressures, some are complicated, difficult to control, have low conversion, are time consuming, etc. Downsides are usually more than one, e.g. sol-gel synthesis [17], which is a typical bottom-up, chemical method, provides very pure products, does not require expensive equipment or harsh conditions, but usually uses relatively expensive alkoxides as precursors and organic solvents. Additionally, the process is not easily controllable and, in order to induce crystallization, thermal treatment is usually required. Combustion synthesis [18], which could also be classified as bottom-up, chemical method, is simple and cheap, but it is accompanied by the emission of a large amount of harmful gases, and the final product is often contaminated with carbon. Mechanochemical synthesis [19], typical physical, i.e. top-down method, requires somewhat more substantial, but still affordable equipment. The process even allows the preparation of metastable phases unattainable by other methods. However, the product is often polydisperse, heavily agglomerated, and may be contaminated with the mill material. Furthermore, the occurrence of structural flows is common. Nor is the hydrothermal process ideal [7], but it is a very useful bottom-up method, often favored by sci-

entific laboratories and industry. According to Byrappa and Tadafumi [20], both being authority for this method, hydrothermal synthesis turned into frontline technology for advanced materials and nanomaterials processing. In their editorial of the special issue of the Journal of Nanomaterials dedicated to the hydrothermal synthesis of nanomaterials, Gan et al. [21] claim that hydrothermal synthesis is one of the most commonly used methods for preparation of nanomaterials.

3. HYDROTHERMAL SYNTHESIS

The term "hydrothermal" was first used by the Scottish geologist Sir Roderick Murchison in the mid-19th century to describe the formation of minerals from aqueous solution at elevated temperatures and pressures in the course of magma cooling [20]. The first to use the hydrothermal method for synthesis was K.E. Schafhäutl [22] who grew a quartz crystal from silicic acid in a pressure vessel. In short, hydrothermal synthesis may be described as a method of producing nanoparticles by chemical reactions in aqueous media at elevated temperatures and pressures [23]. Like any other definition, this one is unilateral, because it neglects the fact that other materials besides nanoparticles, such as powders, coating, single crystals, etc., may be obtained by hydrothermal synthesis. It is furthermore not necessary for the medium to be water, although in such case, the synthesis is usually (but not inevitably) called solvothermal (Figure 6) [24]. For example, Byrappa and Tadafumi [20] define the hydrothermal process as any heterogeneous chemical reaction in the presence of a solvent above room temperature and pressure in a closed system. This definition encompasses all possible processes in which the preparation of nanoparticles and bulk single crystals are the most important ones, aqueous or non-aqueous solvents, different technical performances and approaches, etc. Hydrothermal synthesis is fundamentally based on the fact that the solubility of most inorganic materials increases at elevated temperatures, enabling the dissolution of precursors. Sometimes precursors are completely insoluble at standard temperature and pressure [25]. From these dissolved substances, the desired new crystalline phase crystallizes due to lesser solubility under the given conditions or reduced solubility due to temperature decrease.

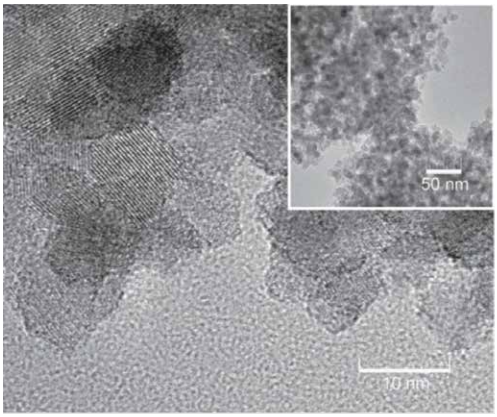

Figure 6. HRTEM micrographs with inset micrograph at lower magnification of solvothermally prepared titanium dioxide nanoparticles with particle size <10 nm. (Reprinted from the publication: S. Kurajica, I. Minga, I. Grčić, V. Mandić, M. Plodinec, The utilization of modified alkoxide as a precursor for solvothermal synthesis of nanocrystalline titania, Materials Chemistry and Physics 196 (2017) 194-204. Copyright (2017), with permission from Elsevier.)

Slika 6. HRTEM mikrografija, s umetnutom mikrografijom pri manjem povećanju, nanočestica titanijevog oksida pripravljenih solvotermalnom sintezom s veličinom čestica <10 nm. (Pretisnuto iz publikacije: S. Kurajica, I. Minga, I. Grčić, V. Mandić, M. Plodinec, The utilization of modified alkoxide as a precursor for solvothermal synthesis of nanocrystalline titania, Materials Chemistry and Physics 196 (2017) 194-204. Copyright (2017), s dopuštenjem Elseviera.)

Hydrothermal methods can be classified in different ways: They may be differentiated according to the purpose of synthesis (bulk and nanomaterials), crystal growth, sintering, deposition, etc. According to temperature processes, hydrothermal methods can be classified into subcritical and supercritical. The ionic product of water (Kw), the equilibrium constant for the self-ionization of water (the reaction between water molecules to produce hydronium, H_3O^+, and hydroxide, OH^-, ions) has a maximum value at about 250–300°C. The hydrothermal synthesis is hence usually carried out below 300°C, which is below the water supercritical point (374°C and 22.1 MPa). However, hydrothermal synthesis above the supercritical point of water has been developed too [25]. According to the production continuity, processes may be divided into: batch process, where the production is accomplished through separate runs; and continuous flow process, where the production is constantly ongoing. The continuous flow hydrothermal synthesis is an option only for the supercritical process. According to the induction of crystallization, the processes of synthesis and crystallization in the autoclave can occur in three ways, based on which the three methods of hydrothermal synthesis are distinguished [26, 27]. The metastable-phase method is based on the difference in solubility between precursors and product. Precursors are thermodynamically less stable under

autoclave conditions and readily dissolve, providing nutrients for crystallization of a stable product from solution. In the temperature-reduction method, the precursors are dissolved at high temperature and pressure, and the temperature is reduced causing supersaturation and crystallization. The temperature difference involves heating the autoclave in such a way that there is a hotter zone at the bottom and a colder zone at the top of autoclave. Reactants are dissolved in the hotter zone and transported to the colder zone by convective motion of the solution occurring due to the temperature gradient. Due to the lower temperature in the upper part, the solution becomes supersaturated, and crystallization occurs. Finally, hydrothermal methods can be improved by a special reactor design, enabling additional ways to transfer the energy required by the system, thus enhancing the process [20, 28, 29].

3.1. Setup and procedure

Hydrothermal synthesis is usually performed in a steel container called an autoclave, or, more precisely, a hydrothermal autoclave reactor, Fig. 7a. This is a steel cylindrical vessel capable of sustaining prolonged high pressure and high temperature without risk of structural damage. Instead of steel, other alloys and even thick glass can be used. The design shown in Fig. 7a is not the only one, but it may be regarded as the most widely used one. Today, there are numerous reactor designs, some of them enabling stirring, fluid redrawing, external gas supply, etc. A Teflon capsule (also called lining) is placed inside the autoclave, although polypropylene, glass, titanium, gold, etc. are sometimes used instead of Teflon. The capsule provides a corrosion-resistant reaction space where the chemical reactions of the hydrothermal process take place. Accordingly, it ought to be chemically inert, i.e. resistant to solvents and chemicals. In most cases, the capsule is of such a shape and size that it fits seamlessly into the interior of the autoclave. Teflon is the most commonly used lining material, since it is resistant to the majority of chemicals and stable at temperatures up to 240°C. However, when Teflon is used, 200°C is considered the maximum safe temperature for synthesis, primarily due to creep to which deformation occurs, but also due to slow thermal degradation, especially during long-term loadings. If Teflon is not suitable due to the required temperature or chemical environment, a capsule made of another material should be used. For some syntheses, the autoclave does not need a lining if the solution is not corrosive to the autoclave material, or if the autoclave material is capable of building a passive layer. The autoclave ought to be easy to assemble and disassemble (Fig. 7b), able to be sealed hermetically, and capable of enduring repeated cycles of temperature and pressure increase and decrease over a long period of time.

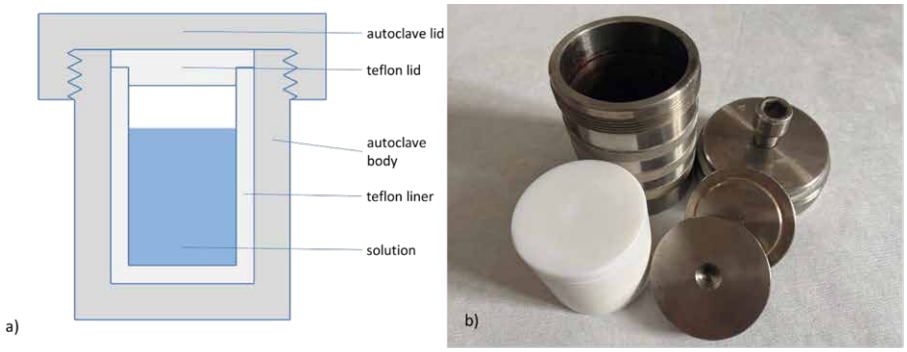

Figure 7. a) Simplified schematic view of the autoclave. b) Autoclave parts and Teflon capsule.
Slika 7. a) Pojednostavljeni shematski prikaz autoklava. b) Dijelovi autoklava i teflonski uložak.

The first step in the synthesis is the preparation of the precursors and the solvent, which are weighted and mixed together [30]. Additional agents, such as mineralizers, surfactants, chelating agents, etc. may be added too [7]. The dissolution of precursors may, but does not need to occur in this step. The solution (or mixture) is then poured into the Teflon capsule, the capsule is placed in the autoclave, and the autoclave is tightly closed to avoid leakage. It is then placed in a device in which the temperature can be easily controlled, e.g. in a laboratory dryer. The temperature is increased to the temperature above water boiling point in order to attain vapor saturation pressure (the pressure at which water vapor is in thermodynamic equilibrium with its condensed state). If the precursors are not easily soluble in the solvent under standard conditions, by changing the conditions, i.e. by increasing the temperature and pressure, their dissolution occurs first. As stated earlier, if the precursors are easily soluble, it means that they had already been dissolved in the solvent. Thereafter, high temperature and pressure conditions facilitate nucleation and consequent growth of nanoparticles. Temperature, pressure and other conditions influence the size and shape of the nanoparticles, so the conditions in this step are adjusted in order to obtain the desired outcome. The process is determined by thermodynamic and kinetic factors, and takes a certain amount of time. Alternatively, nucleation and growth proceed after the decrease of temperature and pressure. After a defined period, the autoclave is removed from the dryer, cooled down and opened. The obtained nanoparticles are separated from the solution. Centrifugation is often necessary for the separation to be accomplished, since fine nanoparticles cannot be separated from the suspension by simple decantation or filtration procedures. If necessary, nano-

particles are washed to remove residual reactants, solvents or byproducts. Water or some other solvent are used, the procedure of washing and separation may be repeated for several times [30]. Finally, the nanoparticles are dried and stored.

3.2. Process control

In order to control the process, the parameters available, i.e. the parameters influencing the outcome of the synthesis, are the following: stoichiometry, solvent, additional agents, temperature, pressure and time [30]. Stoichiometry is important in all chemical processes, because it directly affects the composition of the product. The properties of solvents, such as viscosity or polarity, exert a considerable influence on the process. Solvent interactions with reactants, intermediates and products can affect reaction equilibrium and kinetics, and ultimately affect the products [24]. The solvent, especially water, can participate in the reaction. Under high-temperature and high-pressure hydrothermal conditions, hydrolysis reaction and ion reaction rates naturally increase with water as a medium [29]. Additional agents can be e.g. mineralizers, salts that increase the solubility of precursors through the formation of a solution in which the solubility of precursors is increased, or through the formation of compounds with precursors having greater solubility. Furthermore, as additional agents, chelating agents, reducing the excessive reactivity of precursors and directing the formation of oligomers [24], or surfactants to control the shape and size of the nanoparticles, can be utilized. Temperature controls the thermodynamics and kinetics of product formation. The stability of a certain phase is determined by thermodynamics, while, according to the Arrhenius equation, the reaction rate increases exponentially with the increasing temperature. Temperature considerably reduces the dielectric constant, thus affecting the ability of water to act as a solvent [31]. The increase in water ionization constant with temperature acts beneficially to the reaction rate [29]. Additionally, the reaction rate is accelerated by increasing the probability of molecules colliding. Finally, with the temperature increase, water viscosity decreases, enhancing the mobility of ions or molecules in the solution, thus increasing the crystal growth rate [29]. The temperature is controlled by an external device, such as a laboratory dryer or similar. The pressure is controlled indirectly through the solvent temperature. The pressure influences the solubility and supersaturation, affecting thereby the crystallization process. The pressure also influences the thermodynamic stability of the product, while through water ionization constant, that increases with pressure, the reaction rate increases [29]. The pressure is controlled by the temperature and Teflon capsule fill factor, i.e. the degree of filling of the reaction vessel with the reaction mixture. Considerable vapor pressure exists above the boiling point of water (or other

solvent). Fig. 8 shows the dependence of the pressure on the temperature and the degree of filling with water. Therefore, the greater the temperature and fill factor, the higher the pressure. Most often, the level of filling is 50 to 80%; this corresponds to pressures of 20 to 300 MPa, depending on temperature [32], enabling optimal conditions for hydrothermal synthesis. Finally, the duration of the process affects the product through the kinetics, whereby a short time of the process in the case of slow kinetics favors the obtaining of metastable phases, while thermodynamically stable phases are favored after a longer duration of the process. In addition to the crystallization of the phases, all the factors mentioned above may affect the shape and size of the nanocrystals. However, some additional factors, such as convection inside the autoclave, may influence the process and affect the final product. Additional complexity comes from the fact that the mentioned process parameters interact, i.e. influence each other. Therefore, the impact of process variables on each other and the final product is yet to be fully defined.

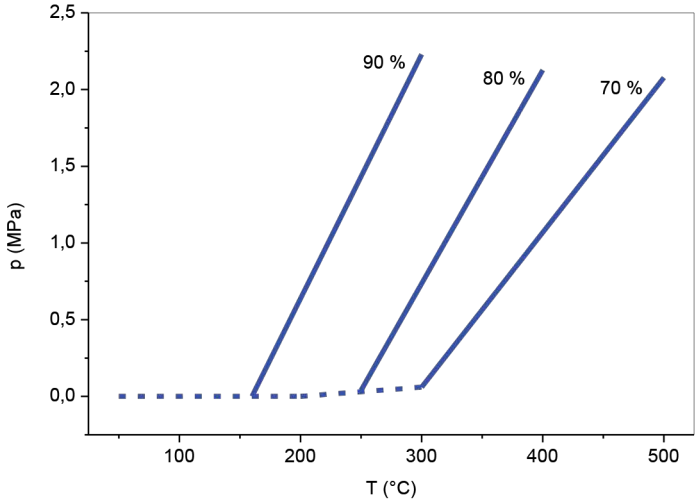

Figure 8. The dependence of pressure on temperature and fill factor (PVT diagram) for the SiO_2-H_2O system, drawn on the basis of data from the publication: G.C. Kennedy, Pressure-volume-temperature relations in water at elevated temperatures and pressures, American Journal of Science, 248 (1950) 540–564.

Slika 8. Ovisnost tlaka o temperaturi i postotku ispunjenosti (PVT dijagram) za sustav SiO_2-H_2O, nacrtana na temelju podataka iz publikacije: G.C. Kennedy, Pressure-volume-temperature relations in water at elevated temperatures and pressures, American Journal of Science, 248 (1950) 540–564.

3.3. The advantages and disadvantages of hydrothermal synthesis

From the economic point of view, hydrothermal synthesis undoubtedly belongs to the affordable group of methods. Steel autoclave and Teflon capsule are to a certain extent more expensive than laboratory glass, but far cheaper than equipment required for other advanced synthesis methods. Solvents and precursors are usually simple chemicals with reasonable prices. Finally, although the process involves prolonged heating of the autoclave, the temperatures are not so high; thus, the process is not considered to be energy demanding. Since water is most commonly used as solvent, relatively harmless precursors are used, temperatures are not so high, the system is closed, its duration is not excessive, and a small amount of waste or no waste at all is generated; it is considered environmentally friendly. Furthermore, it allows compositional, size and shape control of nanoparticles, i.e. the obtaining of pure products, with high crystallinity, small sizes and narrow particle size distribution [21]. Even the control is not too complicated, since most of the parameters can be controlled easily, and their influence on product properties may – if not predicted – be easily determined [20]. Other advantages are that crystalline phases unstable at their melting points and metastable compounds can be obtained via this technique. Finally, the method is versatile, since it can be used for synthesis of a wide range of materials. However, there are downsides to it. If one is aiming to prepare nanoparticles, the concentration of the solution ought not to be high. It follows that the amount of product from one batch will be very small. This shortcoming is reduced by carrying out simultaneous parallel syntheses in multiple autoclaves; however, serious quantities require effort and time. Due to the interdependence of controlling parameters, scale-up is far from being straightforward. Some authors mention the inability to observe the progress of the synthesis as a drawback; however, it is possible today to utilize sensors for this task. Finally yet importantly, high pressures and material fatigue could cause the reactor to explode. In this case, the corrosive solution at high temperatures might be dispersed at high speed, which presents a hazard to human beings.

4. A BRIEF OVERVIEW OF THE AUTHOR'S GROUP ACHIEVMENTS IN HYDROTHERMAL SYNTHESIS

Numerous publications describing hydrothermal syntheses of various materials, especially nanomaterials, and various aspects of hydrothermal processing appear daily. Various nanomaterials, such as metals (noble metals like Au or Ag, magnetic metals like Fe and Co, metal alloys like FePt, etc.) [20, 33, 34], sulphides (such as CdS, PbS, ZnS, CuS, MoS, etc.) [35, 36], various forms of carbon (such as diamond, fullerenes,

carbon nanotubes, etc.), zeolites, hydroxyapatite, semiconductors, composites, etc. [20, 32], are produced using hydrothermal technique. To give an overview of all these studies is a task that might lead to an overabundance of content. Instead, the authors will give a short overview of their own research involving hydrothermal synthesis of ceria nanocrystals.

4.1. Ceria

Both oxides of cerium – cerium(III) oxide (Ce_2O_3) and cerium(IV) oxide (CeO_2) – are called ceria. The more important one, CeO_2, forms a fluorite-type crystal lattice with the space group Fm3m (Figure 9), which is stable over the entire temperature range from room temperature to the melting point at ~ 2400°C.

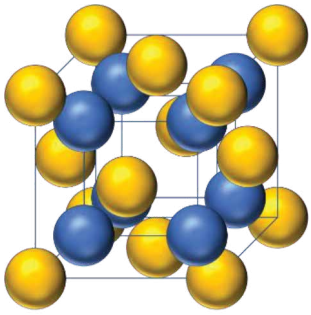

Figure 9. Fluorite crystal lattice of cerium (IV) oxide: Cerium cations (yellow spheres) form a face-centered cubic lattice, while oxygen anions (blue spheres) occupy tetrahedral interstices.
Slika 9. Fluoritna kristalna rešetka cerijevog (IV) oksida: cerijevi kationi (žute kuglice) tvore plošno centriranu kubičnu rešetku, dok anioni kisika (plave kuglice) zauzimaju tetraedarske međuprostore.

Fluorite lattice can withstand a considerable reduction of Ce^{4+} to Ce^{3+} without any change or collapse of the structure, especially at high temperatures [37]. When the partial reduction of Ce^{4+} to Ce^{3+} ions occurs, due to charge compensation, oxygen molecules are released from the crystal lattice, leaving vacancies behind (Figure 10). These vacancies can move within the crystal lattice, and oxygen molecules from the air may be re-adsorbed on them. The good catalytic properties of cerium(IV) oxide are attributed to this easy transition between oxidation states, which enables the formation of oxygen vacancies, easy oxygen mobility through the crystal lattice, and a high oxygen storage capacity within the crystal lattice [38].

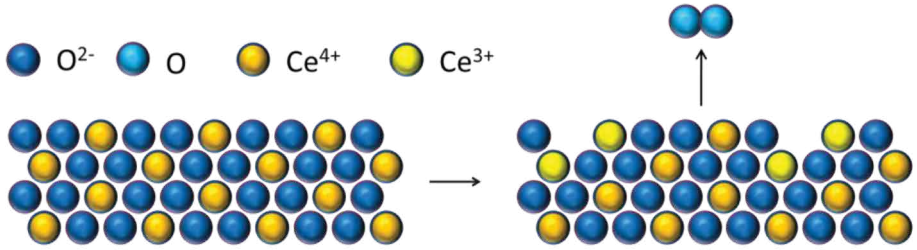

Figure 10. Redox process within cerium(IV) oxide crystal lattice followed by the generation of O_2 molecule and the formation of oxygen vacancies. $Ce^{4+}_{1-x}Ce^{3+}_{x}O_{2-x/2}$ lattice with x/2 oxygen vacancies is formed, and x/4 O_2 molecules are released.

Slika 10. Redoks proces u kristalnoj rešetci cerijeva(IV) oksida praćen stvaranjem molekule O_2 i stvaranjem upražnjenih mjesta koja inače zauzimaju anioni kisika. Nastaje $Ce^{4+}_{1-x}Ce^{3+}_{x}O_{2-x/2}$ rešetka s x/2 slobodnih mjesta kisika i oslobađa se x/4 molekula O_2.

Other important properties of CeO_2 are high mechanical strength, thermal stability and good optical properties. Additionally, due to its wide distribution in the Earth's crust, the price of CeO_2 is relatively low [39]. CeO_2 finds its application in various areas, such as solar cells, fuel cells, supercapacitors, mechanical polishing, sensors, UV protection, and catalysis [40]. Catalytic application is increasingly gaining on importance, since traditional catalysts (precious metals) are expensive, sensitive to high temperatures, and subject to poisoning; alternative solutions are therefore actively sought. It is evident that cerium(IV) oxide has the appropriate properties – low price, lower sensitivity to high temperatures, and resistance to poisoning, while at the same time, it enables achieving high conversions for certain types of chemical processes. Therefore, cerium(IV) oxide is widely used in three-way catalytic converters in automobile exhaust systems, in the conversion of water gas for the purpose of obtaining hydrogen, for various industrial processes, in self-cleaning ovens, and in the removal of air pollutants, such as volatile organic compounds [41, 42, 43, 44].

4.2. Hydrothermal synthesis of ceria nanoparticles

Contemporary researches of hydrothermal and solvothermal synthesis mainly focus on the reactivity of reactants, and the control of reaction conditions and their influence on the structure, morphology and properties of the final product [32]. Our strategy did not deviate from this principle, so we started our research by studying the influence of hydrothermal synthesis conditions influence on the properties of CeO_2 nanoparticles [30]. Our goal was to obtain nanoparticles with the highest specific surface area (SSA),

which is of great importance for catalytic applications. Cerium sulfate tetrahydrate ($Ce(SO_4)_2 \times 4H_2O$) and a concentrated solution of sodium hydroxide (NaOH) were used as precursors, whilst a stainless steel autoclave with a Teflon container was used for the synthesis. The degree of filling of the container with the NaOH solution was 80 %. The process variables that were changed in the experiments were the concentration of NaOH (8 and 12 mol L^{-1}), the amount of $Ce(SO_4)_2 \times 4H_2O$ (0.8 and 1.2 mmol), the duration of the synthesis (16 and 24 h), and the temperature (120 and 180 °C). In order to examine the influence of process parameters on the properties of cerium oxide nanoparticles, i.e. to determine the optimal conditions for obtaining particles with greater SSA, Taguchi's experimental design was used. The SSA was determined using nitrogen adsorption-desorption isotherms. The synthesis temperature was found to be the only significant parameter, where lower temperature enabled the crystallization of nanoparticles with greater SSA (Figure 11). Nanocrystalline ceria with the SSA as great as 226 $m^2 g^{-1}$ was obtained, which was unprecedented for hydrothermally synthesized ceria. X-ray diffraction (XRD) analysis showed that pure cerium(IV) oxide was obtained in all samples, without admixtures or impurities. The crystallite sizes were calculated on the basis of diffraction data utilizing the Scherrer method, and crystallites with sizes as low as 5.9 nm were obtained. Crystallite size turned out to be roughly inversely proportional to the SSA. It was concluded that at a lower temperature, nucleation is favored due to a lower diffusion coefficient, which results in fine particles.

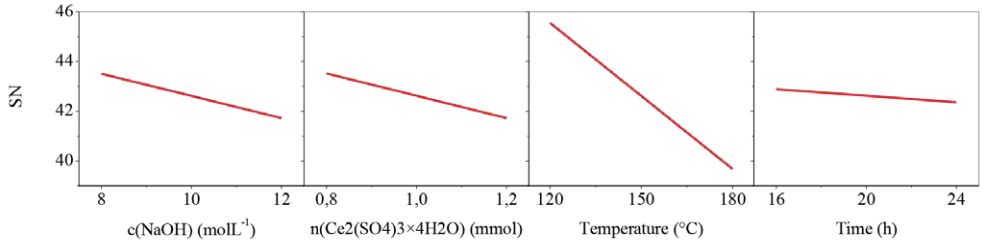

Figure 11. Factor effects plots for each individual factor level (SN – signal to noise ratio). (Reprinted from the publication: S. Kurajica, I. Minga, M. Guliš, V. Mandić, I. Simčić, High Surface Area Ceria Nanoparticles via Hydrothermal Synthesis Experiment Design, J. Nanomater. (2016) 7274949. CC-BY-4.0.)

Slika 11. Dijagrami učinaka čimbenika za različite razine pojedinih čimbenika (SN – omjer signala i šuma). (Pretisnuto iz publikacije: S. Kurajica, I. Minga, M. Guliš, V. Mandić, I. Simčić, High Surface Area Ceria Nanoparticles via Hydrothermal Synthesis Experiment Design, J. Nanomater. (2016) 7274949. CC-BY-4.0.)

Based on previous research, ceria nanocrystals were further prepared under conditions that favor obtaining nanoparticles with high SSA and small crystallite size: 8 M NaOH solution, 0.8 mmol $Ce(SO)_4 \times 4H_2O$, 120 °C and 16 h, degree of filling of 80%. Prepared ceria sample was tested as a potential catalyst for oxidation of volatile organic compounds, using toluene as a model compound [44]. Catalytic tests were performed on ceria previously calcined at 500 °C for 2 h, which caused the increase of the crystallite size to 9 nm. Thermal treatment was inevitable, as the catalytic testing occurs under elevated temperature conditions. Similarly, in practical applications, such as in three-way catalysts, ceria is subjected to high temperatures. The tests showed good catalytic activities for toluene oxidation with temperatures corresponding to 50 % toluene conversion (T_{50}), observed at 250 °C, and even lower temperatures depending on the total flow rate of the gas mixture (Figure 12). The one-dimensional pseudo-homogeneous model of the fixed bed reactor was proposed to describe the reactor performance, and the appropriate kinetic parameters were estimated.

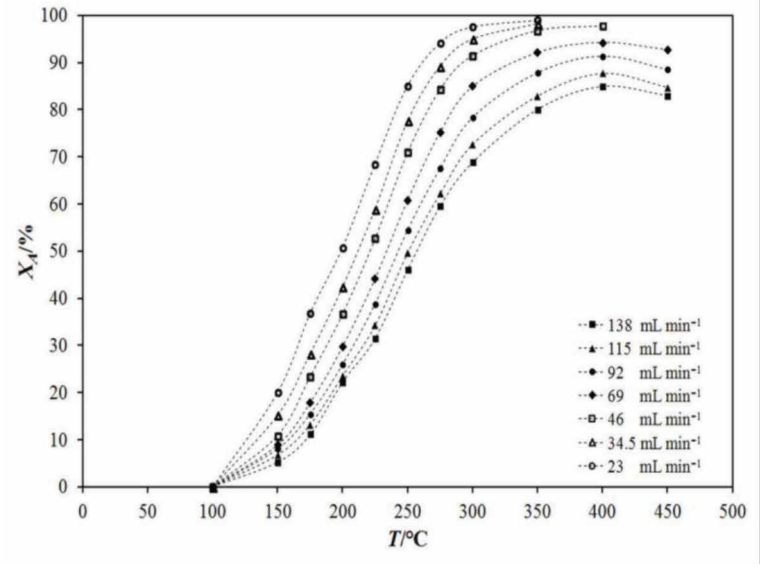

Figure 12. Influence of temperature and total flow rate of the reaction mixture on toluene conversion over CeO_2. (Reprinted from the publication: M. Duplančić, S. Kurajica, V. Tomašić, I. Minga, Catalytic oxidation of toluene on hydrothermally prepared ceria nanocrystals, Chemical and Biochemical Engineering Quarterly, 31 (2017) 375-383. CC-BY-4.0.)

Slika 12. Utjecaj temperature i ukupnog protoka reakcijske smjese preko CeO_2 na konverziju toluena. (Pretisnuto iz publikacije: M. Duplančić, S. Kurajica, V. Tomašić, I. Minga, Catalytic oxidation of toluene on hydrothermally prepared ceria nanocrystals, Chemical and Biochemical Engineering Quarterly, 31 (2017) 375-383. CC-BY-4.0.)

It has been shown that ceria doped with various metal ions can exhibit improved properties [45, 46]. Divalent or trivalent dopants can introduce oxygen vacancies (Figure 13), which in turn affect oxygen mobility, ionic conductivity, and ceria's oxygen storage capacity [47]. Additionally, the synergistic effect between MO_X and CeO_2 promotes electron exchanges between $M^{2+}/M^{(n+1)+}$ and Ce^{3+}/Ce^{4+}. As a result, the combined components undergo oxidation or reduction more easily than their individual counterparts [45]. Furthermore, dopants can influence the crystal growth and morphology of ceria particles, enhancing its sintering properties by stabilizing the crystal size and maintaining or enhancing the specific surface area [47]. Owing to these phenomena, doped CeO_2 often demonstrates higher catalytic activity compared to undoped ceria.

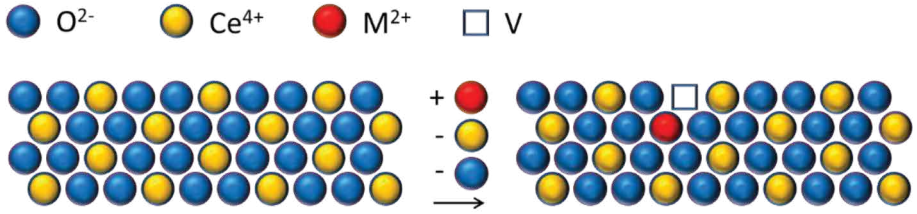

Figure 13. Modification of ceria crystal lattice by substitution of Ce^{4+} ions with metal ions of lower valence. As a consequence of replacement of Ce^{4+} ion with M^{2+} ion, an oxygen vacancy appears.
Slika 13. Modifikacija kristalne rešetke cerijeva(IV) oksida supstitucijom Ce^{4+} s metalnim ionom niže valencije. Kao posljedica zamjene iona Ce^{4+} ionom M^{2+} nastaje upražnjeno mjesto kisika.

Therefore, samples of ceria, substitutionally doped with 10 mol. % of Mn, Fe, Co, Ni, Cu and Zn, were prepared under previously optimized conditions and their properties and catalytic activity were investigated [48]. It was determined that under the synthesis conditions applied, at least some of Mn, Cu and Zn enter the ceria crystal lattice. In other samples, additional crystal phases appeared. The presence of foreign cations did not affect the ceria particle size, crystallite size or the SSA. Particles with particle and crystallite sizes close to 5 nm and the SSA around 200 $m^2\ g^{-1}$ were obtained (Figure 14). However, with the exception of the Mn doped sample, a negative influence of the dopants on coarsening resistance has been noted. Most importantly, it was determined that doping with Cu and Mn considerably enhanced the ceria catalytic activity.

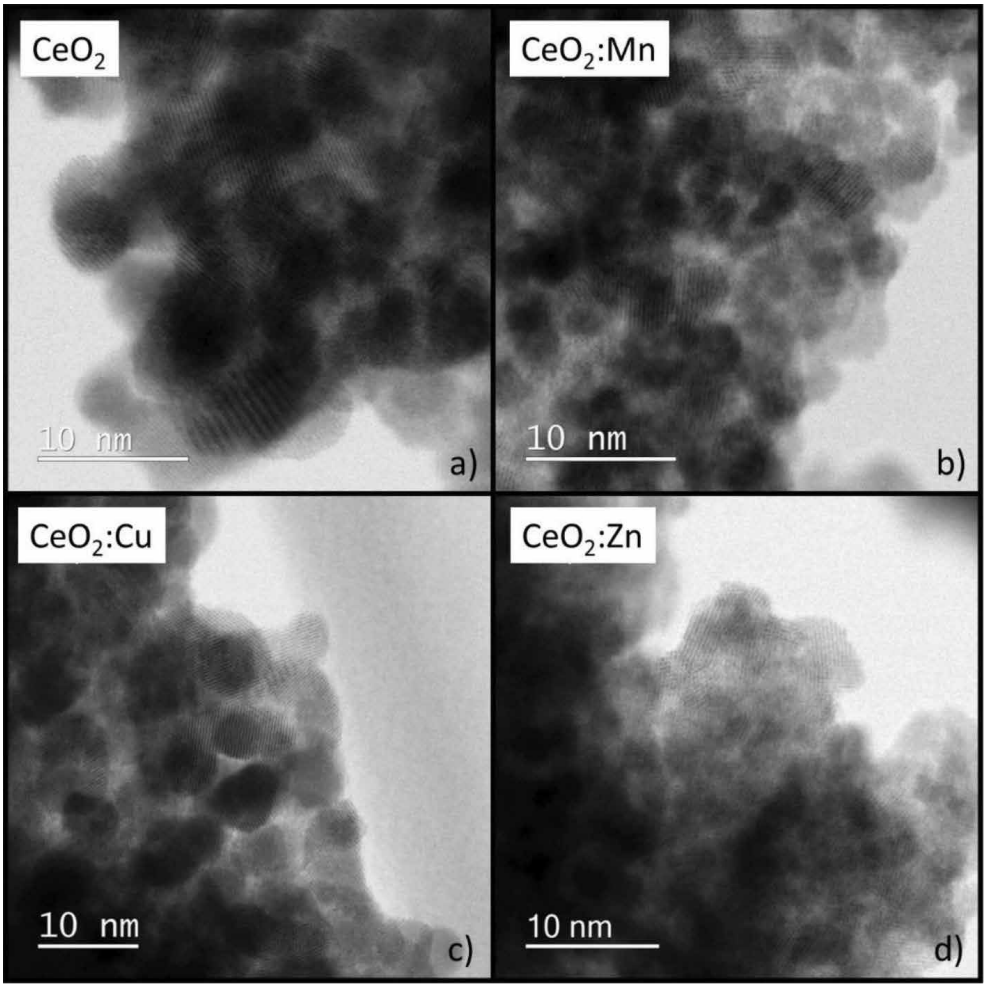

Figure 14. Bright Field STEM micrographs of the as-prepared samples: a) pure ceria, and ceria doped with b) Mn, c) Cu and d) Zn. (Reprinted from the publication: S. Kurajica, K. Mužina, G. Dražić, G. Matijašić, M. Duplančić, V. Mandić, M. *Župančić*, I. K. Munda, A comparative study of hydrothermally derived Mn, Fe, Co, Ni, Cu and Zn doped ceria nanocatalysts, Materials Chemistry and Physics, 244 (2020) 12689. Copyright (2020), with permission from Elsevier.)
Slika 14. STEM mikrografija u svijetlom polju pripravljenih uzoraka: a) čistog cerija i cerija dopiranog s b) Mn, c) Cu i d) Zn. (Pretisnuto iz publikacije: S. Kurajica, K. Mužina, G. Dražić, G. Matijašić, M. Duplančić, V. Mandić, M. Župančić, I. K. Munda, A comparative study of hydrothermally derived Mn, Fe, Co, Ni, Cu and Zn doped ceria nanocatalysts, Materials Chemistry and Physics, 244 (2020) 12689. Copyright (2020), s dopuštenjem Elseviera.)

Since the results for ceria doped with manganese and copper were promising, a more detailed research of ceria doped with these metals was commenced.

Thus, samples with 10, 20 and 30 % of cerium ions replaced with manganese ions have been prepared by hydrothermal synthesis [49]. The XRD analysis revealed that besides ceria, monoclinic birnessite ($Na_{0.55}Mn_2O_4 \times 1.5H_2O$) appears in the samples. Typical layered formations of birnessite, along with ceria nanoparticles, were observed via scanning electron microscope (SEM). Whole powder pattern decomposition (WPPD) enabled the determination of weight percentages, lattice constants and crystallite sizes of ceria, as well as birnessite. The decrease of ceria crystal lattice constant with the increase in Mn loading points out to the entrance of Mn into ceria crystal structure, and the same observation is reinforced by energy dispersive X-ray spectroscopy (EDS). The amount of Mn entering the ceria lattice or forming birnessite varies with nominal composition. Crystallite size and the SSA of pure and Mn doped ceria samples were between 3.1 and 3.4 nm, and 183 and 212 $m^2\ g^{-1}$, respectively. Thermal analysis in combination with the XRD and Fourier-transformed infrared spectroscopy (FTIR) results showed that birnessite decomposes below 200 °C and transforms into a romanechite-like phase, $Na_2Mn_5O_{10}$, with nanorod morphology after thermal treatment at 500 °C for 2 h (Figure 15). Thermogravimetric analysis enabled the calculation of birnessite weight percentage on the basis of the interlayer water loss, confirming the WPPD results.

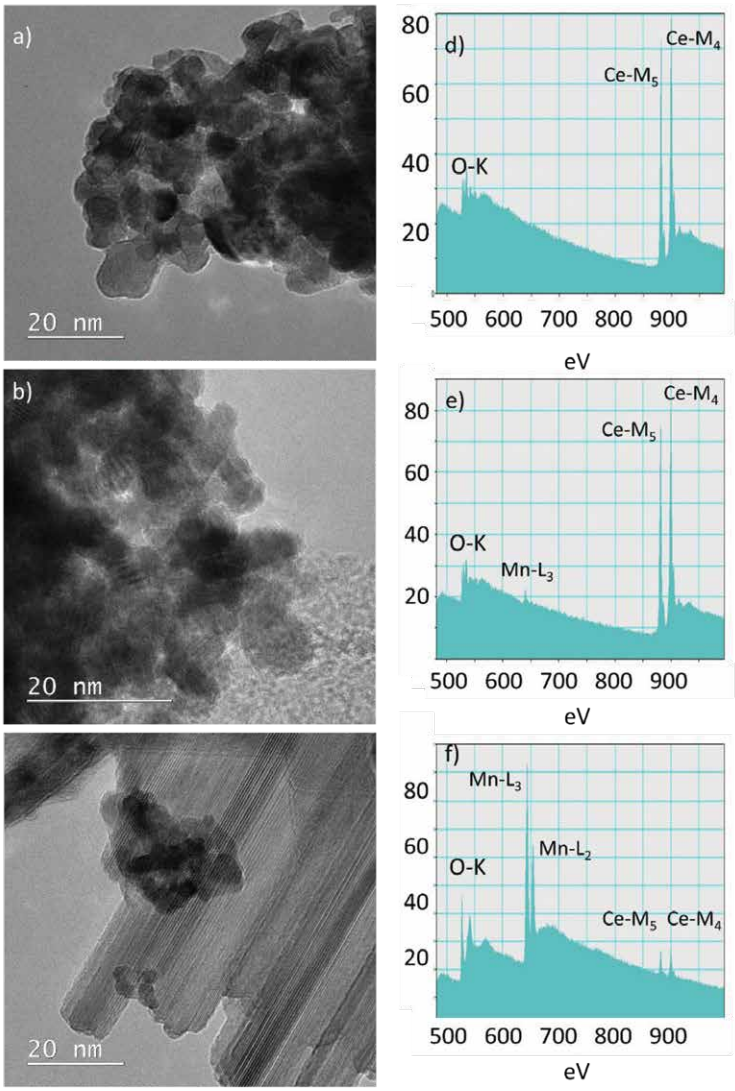

Figure 15. HRTEM micrographs of Mn-doped ceria samples thermally treated at 500 °C for 2 hours. a) Pure sample, b) spherical nanoparticles of the sample doped with 10% Mn, c) fibrous structure of the sample doped with 10% Mn, d) electron energy loss spectroscopy (EELS) of a, e) EELS of b, f) EELS of c. (Reprinted from the publication: S. Kurajica, I. K. Munda, G. Dražić, V. Mandić, K. Mužina, L. Bauer, G. Matijašić, Manganese-doped, hydrothermally-derived ceria: The occurrence of birnessite and the distribution of manganese, Ceramics International, 46 (2020) 29451-29459. Copyright (2020), with permission from Elsevier).

Slika 15. HRTEM mikrografije uzoraka cerija dopiranog s Mn termički tretiranih pri 500 °C tijekom 2 sata. a) čisti uzorak, b) sferične nanočestice uzorka dopiranog s 10% Mn, c) vlaknasta struktura uzorka dopiranog s 10% Mn, d) spektroskopija gubitka energije elektrona (EELS) od a, e) EELS od b, f) EELS od c. (Pretisnuto iz publikacije: S. Kurajica, I. K. Munda, G. Dražić, V. Mandić, K. Mužina, L. Bauer, G. Matijašić, Manganese-doped, hydrothermally-derived ceria: The occurrence of birnessite and the distribution of manganese, Ceramics International, 46 (2020) 29451-29459. Copyright (2020), s dopuštenjem Elseviera.)

Thermal stability of Mn-doped ceria samples was further examined through grain growth kinetics investigation [50]. Samples were isothermally annealed at temperatures between 500 and 700 °C for different annealing times. The crystallite sizes of doped ceria nanoparticles were determined using Scherrer analysis from the XRD data and compared with grain sizes obtained via TEM analysis. Using isothermal and non-isothermal kinetic models, it has been shown that the presence of manganese reduces the grain growth rate of ceria, i.e. that doping with manganese increases ceria thermal stability (Figure 16).

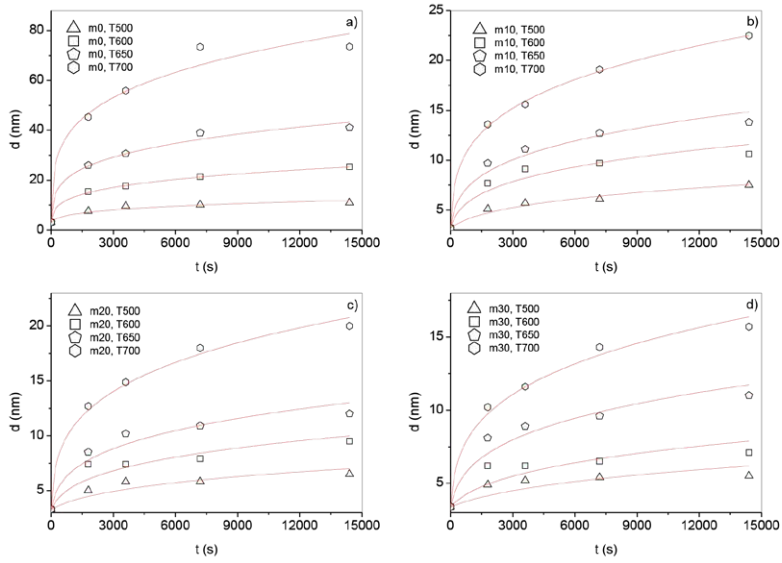

Figure 16. The average crystallite size of: a) pure ceria sample, b) sample doped with 10 mol. % of Mn, c) sample doped with 20 mol. % of Mn, and d) sample doped with 30 mol. % of Mn, thermally treated at various temperatures for various durations. Lines represent the fit of equation. $R_t = (kt + R_0^n)^{1/n}$ to data. (Reprinted from the publication: S. Kurajica, I. K. Munda, F. Brleković, K. Mužina, G. Dražić, J. Šipušić, M. Mihaljević, Manganese-doped ceria nanoparticles grain growth kinetics, Journal of Solid State Chemistry, 291 (2020) 121600. Copyright (2020), with permission from Elsevier.)

Slika 16. Prosječna veličina kristalita: a) uzorka nedopiranog cerijeva oksida, b) uzorka cerijeva oksida dopiranog s 10 mol. % mangana, c) uzorka cerijeva oksida dopiranog s 20 mol. % mangana i d) uzorka cerijeva oksida dopiranog s 30 mol. % mangana, termički obrađenih pri različitim temperaturama u različitom trajanju. Linije predstavljaju slaganje jednadžbe $Rt = (kt + R_0^n)^{1/n}$ s podacima. (Pretisnuto iz publikacije: S. Kurajica, I. K. Munda, F. Brleković, K. Mužina, G. Dražić, J. Šipušić, M. Mihaljević, Manganese-doped ceria nanoparticles grain growth kinetics, Journal of Solid State Chemistry, 291 (2020) 121600. Copyright (2020), s dopuštenjem Elseviera.)

Finally, phase composition, morphology, properties and catalytic activity of hydrothermally-derived manganese-doped ceria nanoparticles thermally treated at 500 °C for 2 h were investigated [51]. Nanocrystalline ceria was the main phase in all the samples, while the XRD revealed the presence of $Na_2Mn_5O_{10}$ only in the sample doped with 30 mol.% of Mn. However, TEM coupled with the EDS exposed the presence of the same phase in the sample doped with 20 mol.% Mn. Ceria particles showed spherical morphology and particle sizes ranging from 4.3 to 9.2 nm, while the $Na_2Mn_5O_{10}$ phase displayed tubular morphology with a length of at least 1 μm (Figure 17). The fact that a substantial amount of manganese entered the ceria crystal lattice was confirmed through the decrease of ceria lattice constant and the EDS spectra of the ceria nanoparticles. Beneficial impact of manganese doping on the SSA of ceria was observed too. Additionally, the decrease in the Ce^{3+} content and a drastic increase in adsorbed oxygen with an increase in the Mn load was revealed by X-ray photoelectron spectroscopy (XPS) (Figure 17). The decrease in the Ce^{3+} content was a consequence of replacing cerium ions with Mn^{3+}, while adsorbed oxygen increase is the consequence of Mn^{3+} species promoting oxygen migrations to the surface of the sample. Finally yet importantly, in comparison with the pure sample, the doped samples showed a considerably higher catalytic activity for the process of toluene oxidation.

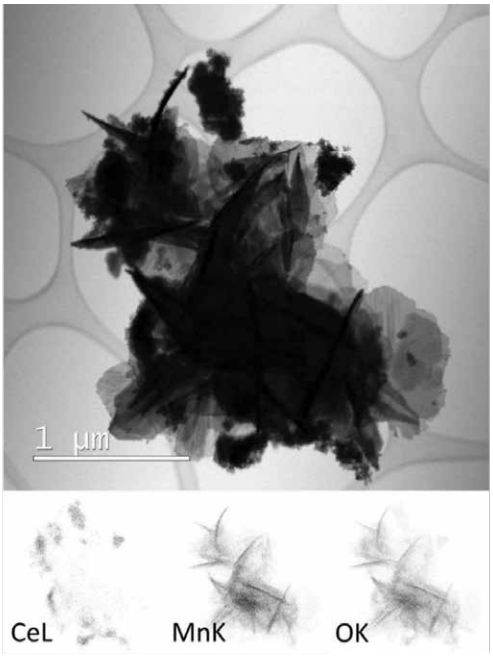

Figure 17. TEM micrograph of secondary phase in: 20 mol.% Mn doped sample, EDS elemental (Ce, Mn and O) distribution maps are given below. (Reprinted from the publication: S. Kurajica, I. K. Ivković, G. Dražić, V. Shvalya, M. Duplančić, G. Matijašić, U. Cvelbar, K. Mužina, Phase composition, morphology, properties and improved catalytic activity of hydrothermally-derived manganese-doped ceria nanoparticles, Nanotechnology, 33 (2022) 135709. CC-BY-4.0.)

Slika 17. TEM mikrografija sekundarne faze u: uzorku dopiranom s 20 mol.% Mn, EDS mape distribucije elemenata (Ce, Mn i O) dane su ispod glavne slike. (Pretisnuto iz publikacije: S. Kurajica, I. K. Ivković, G. Dražić, V. Shvalya, M. Duplančić, G. Matijašić, U. Cvelbar, K. Mužina, Phase composition, morphology, properties and improved catalytic activity of hydrothermally-derived manganese-doped ceria nanoparticles, Nanotechnology, 33 (2022) 135709. CC-BY-4.0.)

Mn-doped ceria was further researched using other synthesis methods, such as sol-gel [17] and mechanochemical synthesis [19]. These studies will however not be presented here.

Besides Mn-doped ceria, Cu-doped ceria was rated as promising, so the research of these samples was accomplished too. Thus, hydrothermally derived ceria nanoparticles doped with copper with nominal composition given by the formula: $Cu_xCe_{1-x}O_2$, where $x = 0$, 0.1, 0.2, 0.3, 0.4, and 0.5, respectively, were prepared [52]. According to the XRD analysis, besides ceria, no additional phases were formed for all samples up to $x = 0.4$. On the other hand, inductively coupled plasma mass spectrometry (ICP-MS) and the EDS analyses showed copper incorporation in ceria crystal lattice in far lower amounts than nominal. Nevertheless, it has been shown that incorporated copper has a considerable influence on the ceria properties. The size of nanoparticles determined by TEM decreases with the increase of copper load from 6 nm for the pure sample to 3.8 nm for the 40 mol. % doped sample (Figure 18). The increase in copper loading also caused the reduction of the band gap determined by the UV-Vis diffuse reflectance analysis (UV–Vis DRS), and an increase in reducibility, as proven by temperature programmed reduction by hydrogen (H_2-TPR).

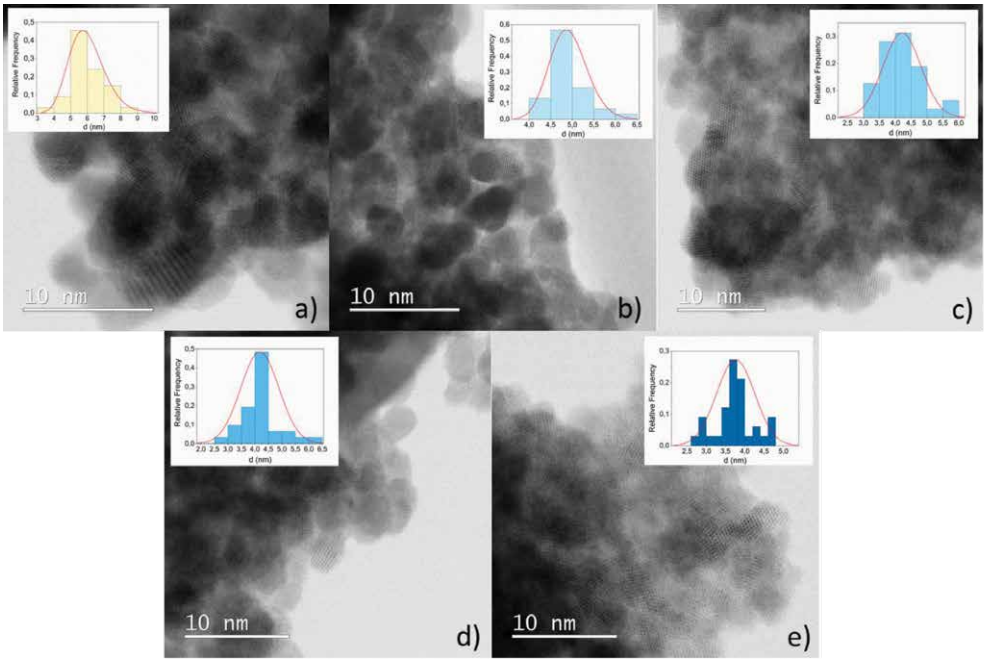

Figure 18. HRTEM micrographs and particle size distributions of a) pure ceria, b) 10 mol. % Cu, c) 20 mol. % Cu, d) 30 mol. % Cu, and e) 40 mol. % Cu doped ceria. Particle size distributions were based on 30 analyzed particles for each sample. (Reprinted from the publication: K. Mužina, S. Kurajica, G. Dražić, P. Guggenberger, G. Matijašić¸ True doping levels in hydrothermally derived copper-doped ceria, Journal of Nanoparticle Research, 23 (2021) 149. Copyright (2021), with permission from Springer.)

Slika 18. HRTEM mikrografije i raspodjele veličine čestica a) čistog cerijeva(IV) oksida te cerijeva(IV) oksida dopiranog s b) 10 mol. % Cu, c) 20 mol. % Cu, d) 30 mol. % Cu, i e) 40 mol. % Cu (e). Raspodjela veličine čestica temelji se na 30 analiziranih čestica za svaki uzorak. (Pretisnuto iz publikacije: K. Mužina, S. Kurajica, G. Dražić, P. Guggenberger, G. Matijašić¸ True doping levels in hydrothermally derived copper-doped ceria, Journal of Nanoparticle Research, 23 (2021) 149. Copyright (2021), s dopuštenjem Springera.)

The catalytic application of ceria nanoparticles requires their use at elevated temperatures that can cause particle agglomeration and aggregation, diminishing the favorable properties of ceria. Doping might increase the thermal stability of ceria nanoparticles, so copper-doped ceria samples were subjected to the investigation of grain growth kinetics [53]. Pure ceria and ceria doped with 10, 20, 30 and 40 mol.% Cu were thermally treated at temperatures in the range between 300 and 700 °C at various annealing times,

and analyzed by X-ray diffraction analysis and transmission electron microscopy. It has been determined that the addition of copper has a positive influence on ceria thermal stability up to 650 °C, and that the sample with 40 mol.% copper has the greatest stability (Figure 19). Different grain growth regimes in dependence on the temperature range were observed. As the treatment temperature increased, an increase in activation energies and a decrease in grain growth exponents were observed. This behavior was explained through the change in the growth mechanism from diffusion to Ostwald ripening.

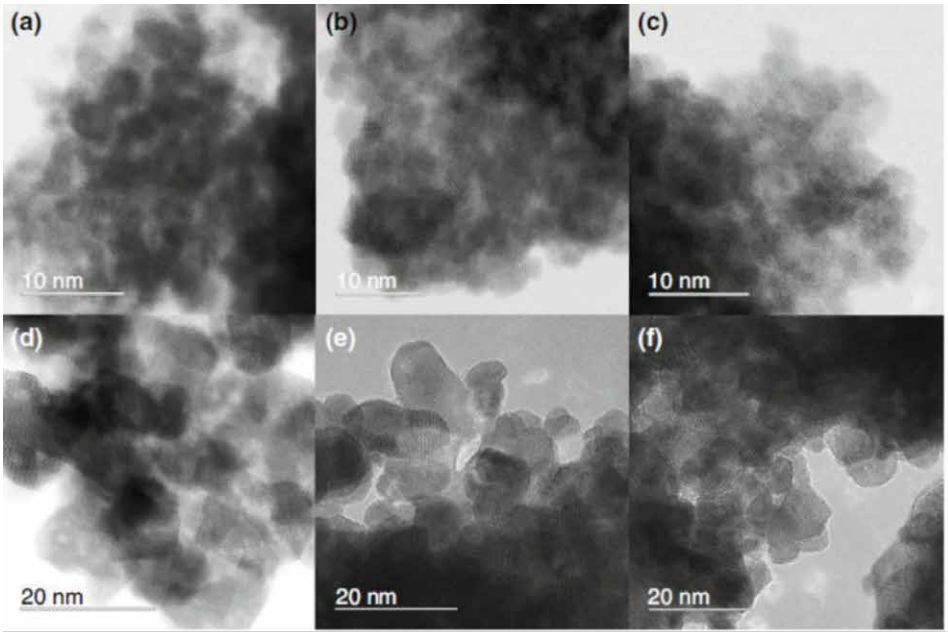

Figure 19. BF-STEM micrographs of (a) pure ceria, (b) 20, and (c) 40 mol.% Cu-doped as prepared samples and (d) pure ceria, (e) 20, and (f) 40 mol.% Cu-doped ceria samples thermally treated at 500 °C for 2 hours. (Reprinted from the publication: K. Mužina, S. Kurajica, F. Brleković, D. Jozić, G. Dražić, L. Volf, H. Bach-Rojecky, Thermal stability study of hydrothermally derived copper-doped cerium (IV) oxide nanoparticles, Journal of Thermal Analysis and Calorimetry, 148 (2023) 1657-1667. Copyright (2023), with permission from Springer.)

Slika 19. BF-STEM mikrografije (a) čistog uzorka cerijeva(IV) oksida i uzoraka cerijeva(IV) oksida dopiranih s (b) 20 i (c) 40 mol.% Cu, koji nisu termički obrađeni, te (d) čistog uzorka cerijeva(IV) oksida i uzoraka cerijeva(IV) oksida dopiranih s (e) 20 i (f) 40 mol.% Cu (c) termički obrađenih pri 500 °C tijekom 2 sata. (Pretisnuto iz publikacije: K. Mužina, S. Kurajica, F. Brleković, D. Jozić, G. Dražić, L. Volf, H. Bach-Rojecky, Thermal stability study of hydrothermally derived copper-doped cerium (IV) oxide nanoparticles, Journal of Thermal Analysis and Calorimetry, 148 (2023) 1657-1667. Copyright (2023), s dopuštenjem Springera.)

Finally, catalytic activity and properties of thermally treated copper-doped ceria nanoparticles in the process of volatile organic compounds oxidation were tested using benzene, toluene, ethylbenzene, and o-xylene [54]. A beneficial synergistic effect between copper and cerium species is visible in the catalytic properties, where the sample with the largest dopant loading exhibited the best catalytic activity for all studied VOCs (Figure 20).

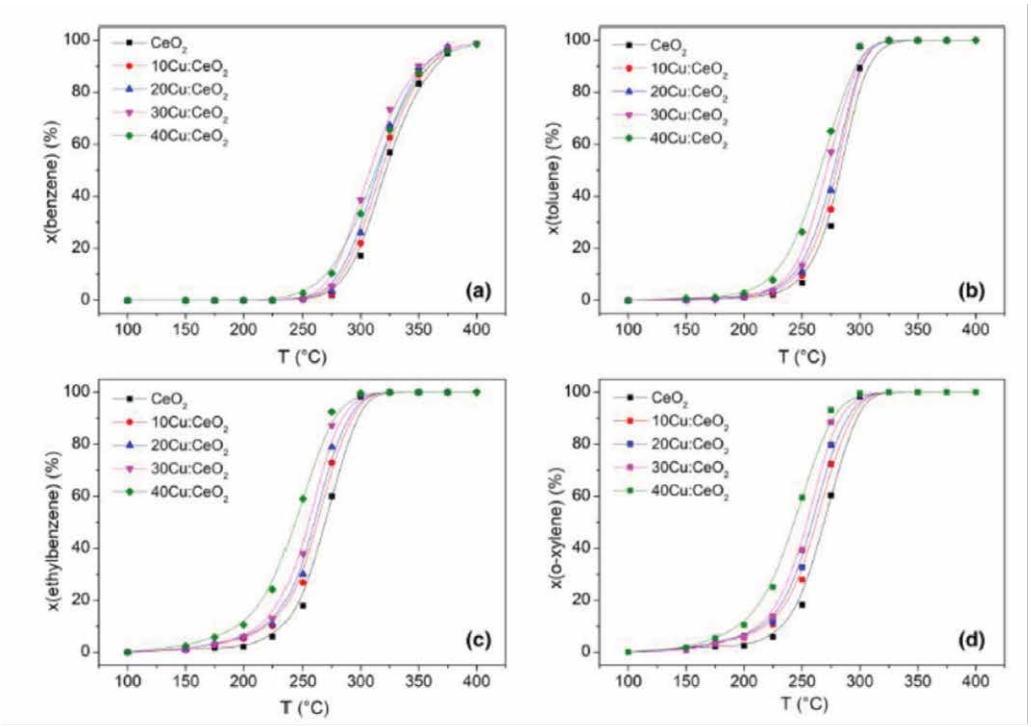

Figure 20. The influence of reactor temperature on conversion of benzene (a), toluene (b), ethylene (c), and o-xylene (d) over pure and Cu-doped ceria nanocatalyst. (Reprinted from the publication: K. Mužina, S. Kurajica, P. Guggenberger, M. Duplančić, G. Dražić, Catalytic activity and properties of copper doped ceria nanocatalyst for VOCs oxidation, Journal of Materials Research 37 (2022) 1929-1940. Copyright (2023), with permission from Springer.)

Slika 20. Utjecaj temperature reaktora na konverziju benzena (a), toluena (b), etilena (c) i o-ksilena (d) preko čistog i Cu-dopiranog cerijevog nanokatalizatora. (Pretisnuto iz publikacije: K. Mužina, S. Kurajica, P. Guggenberger, M. Duplančić, G. Dražić, Catalytic activity and properties of copper doped ceria nanocatalyst for VOCs oxidation, Journal of Materials Research 37 (2022) 1929-1940. Copyright (2023), s dopuštenjem Springera.)

As a kind of spin-off research of hydrothermally-derived doped ceria, a few more investigations were conducted. In the first among them, hydrothermally prepared pure ceria and Zn-doped ceria were tested as candidates for UV filter materials in sunscreens [55]. Fine ceria and doped ceria nanoparticles with particle sizes of 6.1±0.9 and 4.2±0.4 nm, and homogeneous distribution of zinc were obtained. As required, nanoparticles exhibited transparency in the visible region, and absorbance in the UV region, having a band gap of 3.23 and 3.14 eV for pure and doped sample, respectively. For the oxidation stability time determination, the Castor oil oxidation process was utilized. Rather satisfactory results of 23 hours for the pure and 15 hours for the doped sample were obtained. Finally, the *in vitro* cytotoxicity study showed good tolerance of human skin keratinocytes (HaCaT cell line) to prepared nanoparticles, without considerable differences in the skin cells viability (Figure 21).

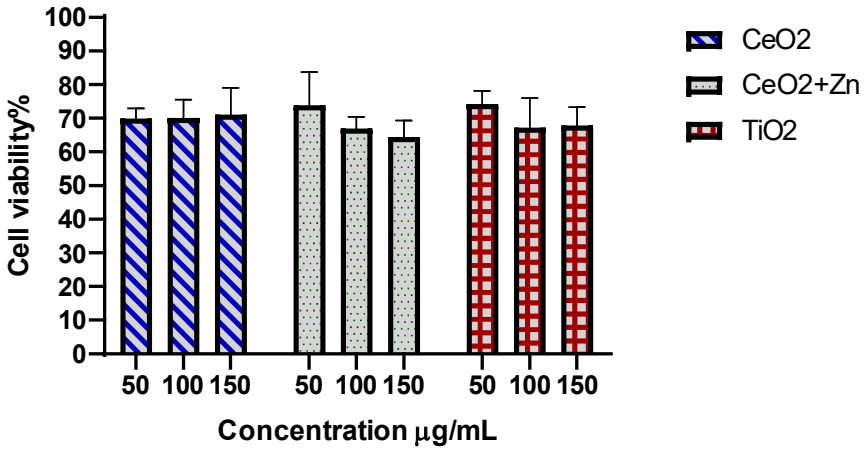

Figure 21. HaCaT cells viability (%) after 24 h of incubation at 37 °C treated with ceria, zinc-doped ceria, and titania nanoparticles as determined by the MTT assay. The values denote the mean ± S.D. (n = 6). (Reprinted from the publication: S. Kurajica, K. Mužina, S. Keser, G. Dražić, I. K. Munda, Assesment of cell toxicity and oxidation catalytic activity of nanosized zinc-doped ceria UV filters, CABEQ, 35 (2021) 157-164. CC-BY-4.0.)

Slika 21. MTT testom određena vijabilnost stanica HaCaT (%) nakon 24 sata inkubacije pri 37 °C tretiranih cerijevim, cinkom dopiranim cerijevim i titanijevim nanočesticama. Prikazane su srednje vrijednosti ± S.D. (n = 6). (Pretisnuto iz publikacije: S. Kurajica, K. Mužina, S. Keser, G. Dražić, I. K. Munda, Assesment of cell toxicity and oxidation catalytic activity of nanosized zinc-doped ceria UV filters, CABEQ, 35 (2021) 157-164. CC-BY-4.0.)

In another study, ceria nanoparticle slurry was tape-casted onto a conducting glass substrate to form thin-films of various thicknesses, and investigated as humidity sensor [12]. The last investigation published, having some continuity with the described research, deals with the combustion synthesis of zirconium-doped ceria nanocatalyst [56]. Since in these investigations, the methods of sample preparation were coprecipitation and combustion synthesis, we will not further comment them here.

We are currently at the beginning of research in which we intend to use nanocasting as a synthesis method, i.e. mesoporous doped ceria will be prepared via the hard template method. Although it seems that we are diverging from hydrothermal synthesis, it is highly probable that our group will continue research on the materials prepared by hydrothermal synthesis.

5. CONCLUSION

It has been shown that the hydrothermal synthesis is an efficient method for the preparation of nanoparticles of various materials. The main advantages of this method are simplicity, low cost and environmental acceptability in terms of precursors, equipment and energy consumption, the possibility of good control of the properties of the obtained product by changing the internal and external process parameters, and the purity and homogeneity of the final product. It has been clearly shown at the example of doped cerium oxide that hydrothermal synthesis enables the obtaining of doped cerium oxide nanoparticles of high purity and homogeneity, small in size, with great SSA, etc. It has furthermore been shown that good control of the properties of the obtained materials can be achieved.

In the future, further development of this method may be expected in terms of both the synthesis and the control of synthesis parameters, and in terms of obtaining new materials with new morphologies and properties. Synthesis could move in the direction of continuous synthesis and acceleration of processes rates, while control could go toward *in situ* observation techniques. There is a great demand for nanomaterials in various fields, medicine being one of the prominent ones. Thus, one could expect hydrothermal processing of nanoparticles for utilization in diagnostics and therapy. However, a great variety of other advanced nanomaterials, alloys, semiconductors, metal oxides, composites, etc. could be made possible via the hydrothermal synthesis. New additives could possibly bring better control of shapes, and ultimately result in the creation of materials with new morphologies. Finally, further process enhancement by combination with ultrasonic or microwave energy can be expected.

ACKNOWLEDGEMENTS

The Croatian Science Foundation financed most of the investigations mentioned under the project IP-01-2018-2963. We are much obliged to the Croatian Science Foundation. We furthermore gratefully acknowledge the aegis of the University of Zagreb through research grants. Sincere thanks to project collaborators G. Matijašić, J. Šipušić, M. Duplančić and I. K. Ivković, as well as contributing colleagues V. Mandić, V. Tomašić, F. Faraguna, I. Panžić, L. Bauer, F. Brleković, I. Minga and A. Bafti from the University of Zagreb, Faculty of Chemical Engineering and Technology, Zagreb, Croatia. Our thanks for their valuable contribution go to G. Dražić, National Institute of Chemistry, Ljubljana, Slovenia; P. Guggenberger, University of Vienna, Faculty of Chemistry, Vienna Austria; M. Župančić, Leibniz-Institut für Kristallzüchtung, Berlin, Germany; S. Kesser, University of Zagreb, Faculty of Pharmacy and Biochemistry, Zagreb, Croatia; I. Simčić, Pliva Croatia Ltd., Zagreb, Croatia; D. Jozić, University of Split, Faculty of Chemistry and Technology, Split, Croatia; V. Shvalya, U. Cvelbar, Jožef Stefan Institute, Ljubljana, Slovenia; L. Pavić, D. Kralj, Ruđer Bošković Institute, Zagreb, Croatia and Z. Shi, Hangzhou Dianzi University, College of Materials and Environmental Engineering, Hangzhou, China. Finally, we express our thanks to the following hardworking students: M. Mihaljević, J.-S. Pavelić, L. Volf, H. Bach-Rojecky, T. Grbešić and E. E. Alić, University of Zagreb, Faculty of Chemical Engineering and Technology, Zagreb, Croatia.

References

1. S. Kurajica, S. Lučić Blagojević, Uvod u nanotehnologiju, Hrvatsko društvo kemijskih inženjera i tehnologa, Zagreb, 2017.
2. J. C. Rendón-Angeles, G. Seong, Editorial for the Special Issue: "Hydrothermal Synthesis of Nanoparticles", Nanomaterials 13 (2023) 1463.
3. Nanoscience and nanotechnologies: opportunities and uncertainties, The Royal Society and Royal Academy of Engineering's report on nanotechnologies, 2004., https://royalsociety.org/-/media/policy/publications/2004/9693.pdf
4. B. Mekuye, B. Abera, Nanomaterials: An overview of synthesis, classification,char acterization, and applications, Nano Select 4 (2023) 486–501.
5. I. K. Ivković, S. Kurajica, K. Mužina, I. Čanić, SnO_2 quantum dots prepared utilizing bubbling air, to be published.
6. S. Kurajica, T. Očko, V. Mandić, V. Cigula Kurajica, I. Lozić, Properties and antimicrobial activity of nanosilver deposited cotton fabric coated with γ-methacryloxypropyl trimetoxysilane, J. Nano. Res., 20 (2012) 77-88.

7. S. Kurajica, I. Grčić, I. Minga, V. Mandić, K. Mužina, Hydrothermally-Derived Silver-Decorated Nanocrystalline Anatase Photocatalyst for Reactive Violet 2 Photodegradation, Processes, 11 (2023) 210.
8. V. Mandić, S. Kurajica, M. Plodinec, I. Panžić, Thermal stability and utilization of 1D-nanostructured Co_3O_4 rods derived by simple solvothermal process, Catalysts 12 (2022) 1162.
9. S. Kurajica, M. Vuković Domanovac, K. Mužina, Polyol synthesis of Ag nanowires and biocidal activity of the obtained product, MJCCA 42 (2023) 1-8.
10. S. Kurajica, J. Macan, V. Mandić, M. Galjer, K. Mužina, J. R. Plaisier, Reinforcing blade-cast photocatalytic titania thin film by titanate nanotubes, Materials Research Bulletin, 105 (2018) 142-148.
11. S. Kurajica, V. Mandić, I. Panžić, M. Gaboardi , K. Mužina , A. Lozančić , J. Šipušić, I. K. Munda , L. Višić , S. Lučić Blagojević, L. Gigli , J. R. Plaisier, In-operando diffraction and spectroscopic evaluation of pure, Zr-, and Ce-doped vanadium dioxide thermochromic films derived via glycolate synthesis, Nanomaterials, 10 (2020) 2537.
12. V. Mandić, A. Bafti, L. Pavić, I. Panžić, S. Kurajica, J.-S. Pavelić, Z. Shi, K. Mužina, I. K. Ivković, Humidity sensing ceria thin-films, Nanomaterials 12 (2022) 521.
13. S. Kurajica, J. Šipušić, M. Zupancic, Igor Brautovic, M. Albrecht, ZnO-Al_2O_3-SiO_2 glass ceramics: Influence of composition on crystal phases, crystallite size and appearance, J Non-Cryst. Solids, 553 (2021) 120481.
14. S. Kurajica, J. Schmauch, E. Tkalčec, Application of Numerical Method for the Analysis of Metglas 2826 MB Crystallization Kinetics, Croatica Chemica Acta, 75 (2002) 693-699.
15. S. Kumari, S. Raturi, S. Kulshrestha, K. Chauhan, S. Dhingra, A. Kovacs, K. Thu, R. Khargotra, T. Singh, A comprehensive review on various techniques used for synthesizing nanoparticles, J. Mat. Res Tech. 27 (2023) 1739-1763.
16. N. Abid, A. M. Khan, S. Shujait, K. Chaudhary, M. Ikram, M. Imran, J. Haider, M. Khan, Q. Khan, M. Maqbool, Synthesis of nanomaterials using various top-down and bottom-up approaches, influencing factors, advantages, and disadvantages: a review. Adv Colloid Interface Sci 300 (2021) 102597.
17. S. Kurajica, I. K. Ivković, K. Mužina, V. Mandić, I. Panžić, G. Matijašić, E. E. Alić, Sol-gel synthesis of manganese-doped ceria from acatylacetonate precursors, Journal of Sol-Gel Science and Technology, 101 (2022) 256-268.
18. S. Kurajica, K. Mužina, L. Bauer, F. Brleković, Single-step combustion synthesis of cerium aluminate in the presence of copper, Journal of Materials Engineering and Performance, (2024) DOI: 10.1007/s11665-024-09384-9

19. I. K. Ivković, S. Kurajica, M. Duplančić, F. Faraguna, T. Grbešić, Properties and potential applications of manganese-doped ceria gained by mechanochemical synthesis, ChemistrySelect, 7 (2022) e202104181
20. K. Byrappa, A. Tadafumi, Hydrothermal technology for nanotechnology, Progress in Crystal Growth and Characterization of Materials 53.2 (2007): 117-166.
21. Y. X. Gan, A. H. Jayatissa, Z. Yu, X. Chen, M. Li, Hydrothermal Synthesis of Nanomaterials, Journal of Nanomaterials (2020) 8917013
22. K. F. E. Schafhäutl, Gelehrte Anzeigen Bayer, Akal. 20 (1845) 557, 569, 575, 592.
23. O. Schäf, H. Ghobarkar, P. Knauth, Hydrothermal Synthesis of Nanomaterials, In P. Knauth, J. Schoonman, Eds.,Nanostructured Materials: Selected Synthesis Methods, Properties and Applications, Kluwer, Boston, 2002
24. S. Kurajica, I. Minga, I. Grčić, V. Mandić, M. Plodinec, The utilization of modified alkoxide as a precursor for solvothermal synthesis of nanocrystalline titania, Materials Chemistry and Physics 196 (2017) 194-204.
25. H. Hayashi, Y. Hakuta, Hydrothermal Synthesis of Metal Oxide Nanoparticles in Supercritical Water, Materials 3 (2010) 3794-3817.
26. G. Demazeau, Review. Solvothermal processes: Definition, key factors, governing the involved chemical reactions and new trends, Zeitschrift *für* Naturforschung *B*, 65 (2010) 999-1006.
27. C. S. Cundy, P. A. Cox, Hydrothermal synthesis of zeolites: Precursors, intermediates, and reaction mechanisms, Microporous and Mesoporous Materials, 82 (2005) 1-78.
28. R. Roy, Accelerating the Kinetics of Low-Temperature Inorganic Syntheses, J. Solid State Chem. 111 (1994) 11-17.
29. G. Yang, S.-J. Park, Conventional and Microwave Hydrothermal Synthesis and Application of Functional Materials: A Review, Materials 12 (2019) 1177
30. S. Kurajica, I, Minga, M. Guliš, V. Mandić, I. Simčić, High surface area ceria nanoparticles via hydrothermal synthesis experimental design, Journal of Nanomaterials, (2016) Aricle ID 7274949
31. R. J. White, R. Luque, V. L.Budarin, J. H. Clark, D. J. Macquarrie, Supported metal nanoparticles on porous materials. Methods and applications. Chem. Soc. Rev. 38 (2009) 481–494.
32. S.-H. Feng, G.-H. Li, Chapter 4: Hydrothermal and Solvothermal Syntheses, in Modern Inorganic Synthetic Chemistry, Elsevier, 2017, 73-104.
33. Q. Xie, Z. Dai, W. Huang, J. Liang, C. Jiang, Y. T. Qian, Synthesis of ferromagnetic single-crystalline cobalt nanobelts via a surfactant-assisted hydrothermal reduction process, Nanotechnology 16 (2005) 2958.

34. M. Kim, W.-S. Son, K. H. Ahn, D. S. Kim, H.-S. Lee, Y.-W. Lee, Hydrothermal synthesis of metal nanoparticles using glycerol as a reducing agent, The Journal of Supercritical Fluids, 90 (2014) 53-59.
35. P. W. Dunne, C. L. Starkey, M. Gimeno-Fabra, E.H. Lester, The rapid size- and shape-controlled continuous hydrothermal synthesis of metal sulphide nanomaterials, Nanoscale, 6 (2014) 2406-2418.
36. X. Yan, E. Michael, S. Komarneni, J. R. Brownson, Z.-F. Yan, Microwave- and conventional-hydrothermal synthesis of CuS, SnS and ZnS: Optical properties, Ceramics International, 39 (2013) 4757-4763.
37. L. F. Arenas, C. Ponce de León, F. C. Walsh, Electrochemical redox processes involving soluble cerium species, Electrochim. Acta. 205 (2016) 226-247.
38. M. Mogensen, N. M. Sammes, G. A. Tompsett, Physical, chemical and electrochemical properties of pure and doped ceria, Solid State Ion. 129 (2000) 63-94.
39. R. Bakkiyaraj, G. Bharath, K. Hasini Ramsait, A. Abdel-Wahab, E. H. Alsharaeh, S.-M. Chen, M. Balakrishnan, Solution combustion synthesis and physicochemical properties of ultrafine CeO_2 nanoparticles and their photocatalytic activity, RSC Adv. 6 (2016) 51238-51245.
40. I. V.Zagaynov, S. V. Kutsev, Formation of mesoporous nanocrystalline ceria from cerium nitrate, acetate or acetylacetonate, Appl. Nanosci. 4 (2014) 339-345.
41. G. Ramakrishnan, K. Naveen, Emission and dynamic characteristics of three-way catalytic converter by computational fluid dynamics, Int. J. Eng. Sci. 6 (2016) 3503-3510.
42. Z. Ren, F. Peng, J. Li, X. Liang, B. Chen, Morphology-dependent properties of Cu/CeO2 catalysts for the water-gas shift reaction, Catalysts 7 (2017) 48.
43. P. Palmisano, N. Russo, D. Fino, G. Saracco, V. Specchia, P. Faraldi, D. Polverini, L. Arteconi, Doped ceria catalysts for an innovative self-cleaning domestic oven, 21st North American Catalysis Society Meeting 2009, Proceedings 1 (2009) 341-342.
44. M. Duplančić, S. Kurajica, V. Tomašić, I. Minga, Catalytic oxidation of toluene on hydrothermally prepared ceria nanocrystals, Chem. Biochem. Eng. Q. 31 (2017) 375-383.
45. L. Liu, J. Shi, X. Zhang, J. Liu, Flower-Like Mn-doped CeO2 microstructures: synthesis, characterizations, and catalytic properties, J. Chem. 254750 (2015) 1–11.
46. J. Tan, W. Zhang, Y.-H. Lv, A.-L. Xia, Facile preparation of Mn-doped CeO2 submicrorods by composite-hydroxide-salt-mediated approach and their magnetic property, Mater. Res. 16 (2013) 689–694.
47. Lj Kundakovic, M. Flytzani-Stephanopoulos, Cu- and Ag-modified cerium oxide catalysts for methane oxidation, J. Catal. 179 (1998) 203–221.

48. S. Kurajica, K. Mužina, G. Dražić, G. Matijašić, M. Duplančić, V. Mandić, M. *Župančić*, I. K. Munda, A comparative study of hydrothermally derived Mn, Fe, Co, Ni, Cu and Zn doped ceria nanocatalysts, Materials Chemistry and Physics, 244 (2020) 12689.
49. S. Kurajica, I. K. Munda, G. Dražić, V. Mandić, K. Mužina, L. Bauer, G. Matijašić, Manganese-doped, hydrothermally-derived ceria: The occurrence of birnessite and the distribution of manganese, Ceramics International, 46 (2020) 29451-29459.
50. S. Kurajica, I. K. Munda, F. Brleković, K. Mužina, G. Dražić, J. Šipušić, M. Mihaljević, Manganese-doped ceria nanoparticles grain growth kinetics, Journal of Solid State Chemistry, 291 (2020) 121600.
51. S. Kurajica, I. K. Ivković, G. Dražić, V. Shvalya, M. Duplančić, G. Matijašić, U. Cvelbar, K. Mužina, Phase composition, morphology, properties and improved catalytic activity of hydrothermally-derived manganese-doped ceria nanoparticles, Nanotechnology, 33 (2022) 135709.
52. K. Mužina, S. Kurajica, G. Dražić, P. Guggenberger, G. Matijašić,True doping levels in hydrothermally derived copper-doped ceria, Journal of Nanoparticle Research, 23 (2021) 149.
53. K. Mužina, S. Kurajica, F. Brleković, D. Jozić, G. Dražić, L. Volf, H. Bach-Rojecky, Thermal stability study of hydrothermally derived copper-doped cerium (IV) oxide nanoparticles, Journal of Thermal Analysis and Calorimetry, 148 (2023) 1657-1667.
54. K. Mužina, S. Kurajica, P. Guggenberger, M. Duplančić, G. Dražić, Catalytic activity and properties of copper doped ceria nanocatalyst for VOCs oxidation, Journal of Materials Research 37 (2022) 1929-1940.
55. S. Kurajica, K. Mužina, S. Keser, G. Dražić, I. K. Munda, Assesment of cell toxicity and oxidation catalytic activity of nanosized zinc-doped ceria UV filters, CABEQ, 35 (2021) 157-164.
56. K. Mužina, S. Kurajica, H. Bach-Rojecky, F. Brleković, M. Duplančić, Combustion Synthesis of Zirconium-Doped Ceria Nanocatalyst. Crystals 14 (2024) 108.

HIDROTERMALNA SINTEZA NANOMATERIJALA

Sažetak

Nanomaterijali se mogu pripraviti pomoću različitih metoda sinteze poput sol-gel sinteze, sinteze sagorijevanjem, mehanokemijske sinteze, itd. Među brojnim metodama nanosinteze, hidrotermalna sinteza je jedna od najčešće korištenih. Hidrotermalna sinteza može se definirati kao bilo koja heterogena kemijska reakcija u prisutnosti otapala u zatvorenom sustavu pri temperaturi višoj od sobne i tlaku višem od atmosferskog. Razvoj hidrotermalnih tehnika traje već duže od 150 godina, počevši od sinteze makrokristala, preko sinteze konvencionalnih materijala, pa sve do sinteze novih naprednih materijala, posebice nanomaterijala. U ovom radu opisane su temeljne postavke hidrotermalnog eksperimenta i sam postupak hidrotermalne sinteze. Također, razmotreni su parametri pomoću kojih se može upravljati procesom, kao i prednosti i nedostaci hidrotermalne sinteze. Na kraju je dan kratak pregled postignuća znanstvene grupe prvog autora u hidrotermalnoj sintezi cerijeva oksida.

Ključne riječi: hidrotermalna sinteza; nanomaterijali; cerijev oksid.

Stanislav Kurajica
University of Zagreb
Faculty of Chemical Engineering and Technology
Trg Marka Marulića 19, 10000 Zagreb, Croatia
E-mail: stankok@fkit.unizg.hr

Katarina Mužina
University of Zagreb
Faculty of Chemical Engineering and Technology
Trg Marka Marulića 19, 10000 Zagreb, Croatia
E-mail: kmuzina@fkit.unizg.hr